CrossMark

J. Plasma Phys. (2020), *vol*. 86, 905860604 © The Author(s), 2020.
Published by Cambridge University Press
doi:10.1017/S0022377820001348

Chaos in positive ion–negative ion magnetized plasmas

Samiran Ghosh[1],†, **Biplab Maity**[2] **and Swarup Poria**[1]

[1]Department of Applied Mathematics, University of Calcutta, 92, Acharya Prafulla Chandra Road, Kolkata 700009, India

[2]Government General Degree College, Dantan – II, Paschim Medinipur 721445, West Bengal, India

(Received 16 April 2020; revised 28 September 2020; accepted 29 September 2020)

The dynamical behaviour of weakly nonlinear, low-frequency sound waves are investigated in a plasma composed of only positive and negative ions incorporating the effects of a weak external uniform magnetic field. In the plasma model the mass (temperature) of the positive ions is smaller (larger) than that of the negative ions. The dynamics of the nonlinear wave is shown to be governed by a novel nonlinear equation. The stationary plane wave (analytical and numerical) nonlinear analysis on the basis of experimental parameters reveals that the nonlinear wave does have quasi-periodic and chaotic solutions. The Poincarè return map analysis confirms these observed complex structures.

Key words: plasma nonlinear phenomena

1. Introduction

The wide mass differences between electrons and ions in usual electron–ion plasmas gives rise to different time scales which are used to investigate the long and short wavelength collective phenomena. Such scales collapse in plasmas consisting of only positive and negative charged particles of equal masses, which makes this plasma space–time symmetric (Iwamoto 1993; Zank & Greaves 1995; Greaves & Surko 2000; Oohara & Hatakeyama 2005).

However, experimental observations (Intrator, Hershkowitz & Stern 1983; Kim & Merlino 2007; Merlino & Kim 2008) demonstrate the possibility of the generation of two component positive ion–negative ion (PINI) plasmas with different mass [(Ar^+, SF_6^-) and $(K^+, C_7F_{14}^-)$] and temperature in an almost electron-free plasma (where the electron to ion density ratio $<10^{-4}$). This type of PINI plasma is also observed in the lower region of the ionospheric D-layer, polar mesosphere (Ratcliffe 1972; Kelly & Heelis 1989), plasma processing reactors, in neutral beam sources and in low temperature laboratory experiments (Economou 2007).

Presence of a magnetic field makes the plasma anisotropic and the charged particles exhibit rotational motion transverse to the magnetic field due to the Lorentz force. The ion gyro-frequency ($\omega_{c\pm} = eB_0/m_\pm$, $m_\pm$ is the mass of the positive (negative) ion and B_0 is the magnitude of the static magnetic field) plays a decisive role in the collective dynamics

† Email addresses for correspondence: sran_g@yahoo.com, sgappmath@caluniv.ac.in

https://doi.org/10.1017/S0022377820001348 Published online by Cambridge University Press

of PINI plasmas. Unlike the usual electron–ion plasma (where a wide mass difference gives rise to different time scales), in PINI magnetoplasmas both the ions are magnetized and their gyro-radii are comparable so that they can diffuse across the magnetic field with comparable rates and thereby one can expect that the corresponding ambipolar field is relatively small. In general, two types of waves (low-frequency (LF) sound waves and electrostatic ion cyclotron waves/lower-hybrid waves) can be excited in PINI laboratory plasmas (Intrator *et al.* 1983; Kim *et al.* 2013). A drift-like wave can be excited in a PINI plasma in the presence of an ion density gradient perpendicular to the external magnetic field via universal type instability (Kim, Henrich & Merlino 2008; Rosenberg & Merlino 2009, 2013).

The experimentally generated PINI plasma is an ordinary plasma with an unusual mass ratio of ions (unlike electron–ion ordinary plasma) and can exhibit interesting physical phenomena. In case of large amplitude disturbances, the collective dynamics of such plasmas becomes nonlinear. In equal-mass two-component plasmas, theoretical investigations and numerical simulation predict the existence of localized structures (Stenflo, Shukla & Yu 1985; Yu, Shukla & Stenflo 1986; Kourakis, Verheest & Crammer 2007; Moslem, Kourakis & Shukla 2007; Shukla *et al.* 2009; Shukla, Eliasson & Stenflo 2011; Ghosh, Adak & Khan 2014; Adak, Ghosh & Chakrabarti 2015). However, a very few collective nonlinear interactions are investigated in PINI plasmas (Maity, Ghosh & Bharuthram 2015). The nonlinearity of a physical system manifests itself in the form of coherent complex structures. These structures are best understood by the analytical and numerical solutions of the dynamical equations.

The aim of the present work is to investigate by theoretical and computational (on the basis of laboratory plasma parameters) means how the magnetic field introduces complexity in PINI plasmas and controls the weakly nonlinear three-dimensional collective dynamics of LF sound waves. The present analysis reveals that the dynamics of the weakly nonlinear LF sound wave is governed by a novel nonlinear equation. This nonlinear equation is analysed with its full generality by posing it as an autonomous dynamical system in a plane wave to elucidate the different aspects of the complex phase-space dynamics. The nonlinear analysis predicts the existence of quasi-periodic and chaotic dynamics: an aperiodic long-term behaviour in a deterministic system that exhibits sensitive dependence on initial conditions (Strogatz 1994). The observed complex nonlinear structures are confirmed by the Poincarè return map analysis (Lorenz 1963; Molenaar, Clercx & van Heijst 2005). In PINI plasmas, such nonlinear structures are predicted for the first time in the presence of an external uniform magnetic field.

The paper is organized as follows. The plasma model and the linear mode analysis are presented in § 2. The nonlinear equation that governs the dynamics of a weakly nonlinear LF wave in the presence of an external uniform weak magnetic field is derived in § 3. The analytical and numerical solutions are derived and analysed in § 4. The Poincarè return map analysis for the confirmation of the observed complex structures is also provided in this section. Finally, we conclude with physical applications of our results in § 5.

2. The model and LF linear mode analysis

We consider a fully ionized homogeneous electron-free plasma composed of singly charged positive and negative ions. The plasma is quasi-neutral and the quasi-neutrality condition is given by

$$n_{-0} = n_{+0} = n_0 \text{ (say)}, \tag{2.1}$$

where $n_{+(-)0}$ is the equilibrium positive (negative) ion density. The mass of the positive ion (m_+) is smaller than that of the negative ion (m_-), whereas, the temperature of positive ion

https://doi.org/10.1017/S0022377820001348 Published online by Cambridge University Press

(T_+) is higher than that of negative ion (T_-) (Rosenberg & Merlino 2013). In PINI plasma, both the ion species participate in the shielding process and the Debye length (λ_D) is given by

$$\lambda_D = 1\Big/\sqrt{\lambda_{D+}^{-2} + \lambda_{D-}^{-2}} = \sqrt{\frac{\epsilon_0 T}{n_0 e^2}}, \quad T = \frac{T_- T_+}{T_+ + T_-}, \tag{2.2a,b}$$

where, ϵ_0 is the permittivity of the free space, T is the effective temperature and $\lambda_{D\pm}(= (\epsilon_0 T_\pm/(n_0 e^2))^{1/2})$ is the positive (negative) ion Debye length. All the temperatures are in energy units.

The plasma is situated in a uniform external magnetic field $B = B_0\hat{z}$. We consider a parameter region where both the ions are magnetized and experience the Lorentz force. According to the experimental observations (Intrator *et al.* 1983; Kim & Merlino 2007; Merlino & Kim 2008), we assume that the plasma is collisionless and

$$\lambda_{D\pm} \ll \rho_\pm \ll L \Rightarrow \lambda_D \ll \rho_\pm \ll L, \tag{2.3}$$

where $\rho_\pm = V_{T\pm}/\omega_{c\pm}$ is the positive (negative) ion gyro-radius, $V_{T\pm} = \sqrt{T_\pm/m_\pm}$ is the positive (negative) ion thermal velocity, L is the typical macroscopic length scale including large-scale fluctuation wavelength. This physical assumption (2.3) permits fluid formalism to study the macroscopic dynamics of PINI plasmas (Intrator *et al.* 1983). One of the consequences of the assumption (2.3) is that

$$\lambda_{D\pm} \ll \rho_\pm \Leftrightarrow \omega_{c\pm} \ll \omega_{p\pm} \Rightarrow B_0 \ll \left(n_0 m_\pm \epsilon_0^{-1}\right)^{1/2}, \tag{2.4}$$

(where $\omega_{p\pm} = (n_0 e^2/(\epsilon_0 m_\pm))^{1/2}$ is the positive (negative) ion plasma frequency) which is compatible with the typical PINI experimental parameters (Kim *et al.* 2008, 2013; Rosenberg & Merlino 2013). According to (2.4), the magnetic field is assumed to be weak ($\omega_{c\pm} \ll \omega_{p\pm}$). The characteristic time of variation is assumed to be larger than the cyclotron period $2\pi/\omega_{c\pm}$. Thus the collision-free, two fluid basic equations (normalized) are the continuity equations

$$\left.\begin{aligned} \partial_t n_+ + \nabla\cdot(n_+ \boldsymbol{v}_+) = 0, \\ \partial_t n_- + \nabla\cdot(n_- \boldsymbol{v}_-) = 0, \end{aligned}\right\} \tag{2.5}$$

the momentum conservation equations

$$\left.\begin{aligned} M\mathcal{D}_t^+ \boldsymbol{v}_+ = -\nabla\phi - M\Omega_+\hat{z}\times\boldsymbol{v}_+ - \sigma_+\nabla\ln n_+, \\ \mathcal{D}_t^- \boldsymbol{v}_- = \nabla\phi + \Omega_-\hat{z}\times\boldsymbol{v}_- - \sigma_-\nabla\ln n_-, \end{aligned}\right\} \tag{2.6}$$

and Poisson equation

$$\nabla^2\phi = n_- - n_+, \tag{2.7}$$

where $\mathcal{D}_t^\pm \equiv \partial_t + \boldsymbol{v}_\pm\cdot\nabla$, $M = m_+/m_-$, $\sigma_\pm = T_\pm/T$ and $\Omega_\pm = \omega_{c\pm}/\omega_{p-}$. The positive (negative) ion number density ($n_\pm$) and fluid velocity ($\boldsymbol{v}_\pm$) are normalized in units of n_0 and sound speed $(T/m_-)^{1/2}$, respectively. The time and space scales are normalized in units of ω_{p-} and λ_D, respectively. The electrostatic potential (ϕ) is normalized in units of energy T/e.

We are interested in investigating the nonlinear collective dynamics excited by the LF disturbances in PINI magnetoplasmas. Before that, we study the linear characteristics of

https://doi.org/10.1017/S0022377820001348 Published online by Cambridge University Press

LF modes described by the basic equations (2.5)–(2.7). Following the standard procedure, we obtain the general (normalized) dispersion relation as

$$\tilde{k}^2 = \frac{g_+(\tilde{\omega})}{M\tilde{\omega} - \sigma_+ g_+(\tilde{\omega})} - \frac{g_-(\tilde{\omega})}{\tilde{\omega} + \sigma_- g_-(\tilde{\omega})}; \quad g_\pm(\tilde{\omega}) = \pm \frac{\left(\tilde{k}^2\tilde{\omega}^2 - \tilde{k}_\parallel^2 \Omega_\pm^2\right)}{\tilde{\omega}(\tilde{\omega}^2 - \Omega_\pm^2)}, \tag{2.8a,b}$$

where $\tilde{\omega}(= \omega/\omega_{p-})$ is the oscillation frequency, $\tilde{\boldsymbol{k}}(= \boldsymbol{k}\lambda_D)$ is the wavevector, $\tilde{k}^2 = \tilde{k}_\parallel^2 + \tilde{k}_\perp^2$ and $\tilde{k}_\parallel(\tilde{k}_\perp)$ is the wavenumber parallel (perpendicular) to the direction of the magnetic field.

In the vanishing magnetic field limit ($\tilde{k}_\perp \to 0$, i.e. for purely parallel propagation), the dispersion relation (2.8*a*,*b*) in dimensional form reads as

$$1 = \frac{\omega_{p+}^2}{\omega^2 - k_\parallel^2 V_{T+}^2} + \frac{\omega_{p-}^2}{\omega^2 - k_\parallel^2 V_{T-}^2}. \tag{2.9}$$

In typical PINI laboratory plasma (Intrator *et al.* 1983; Kim *et al.* 2008, 2013; Rosenberg & Merlino 2013), $M < 1$, $T_- < T_+ (V_{T-} < V_{T+})$, and hence the LF, long wavelength ($k_\parallel \lambda_{D\pm} \ll 1$) solution of (2.9) is given by (Intrator *et al.* 1983)

$$\omega^2 = \left(\frac{\delta + M}{1 + M}\right) k_\parallel^2 V_{T+}^2 + O\left(k_\parallel \lambda_{D+}\right)^4, \tag{2.10}$$

where $\delta = (V_{T-}/V_{T+})^2$. In the long wavelength limit ($k_\parallel \to 0$), this LF sound wave always travels at a phase velocity,

$$V_p \left(= \frac{\omega}{k_\parallel}\right) \sim \sqrt{\frac{\delta + M}{1 + M}}, \quad V_{T+} = \sqrt{\frac{1 + T_+/T_-}{1 + M}}, \quad V_{T-} = \sqrt{\frac{T_+ + T_-}{m_+ + m_-}}, \tag{2.11a–c}$$

larger than the thermal velocity of the heavier ions for $T_+ > T_-$ and $m_+ < m_-$. This mode can propagate with negligible Landau damping only if

$$k_\parallel V_{T-} \ll \omega \ll k_\parallel V_{T+} \Leftrightarrow \sqrt{T_-/T_+} \ll \sqrt{m_-/m_+}. \tag{2.12}$$

As long as this condition (2.12) is satisfied, there is a non-trivial range of wavenumbers at which both the ions are non-resonant so that Landau damping is very weak and the LF sound wave (2.11*a–c*) may propagate in PINI plasmas.

Finally, in case of almost perpendicular propagation ($\tilde{k}_\parallel \ll \tilde{k}_\perp$), the dispersion relation (2.8*a*,*b*) in dimensional form reads as

$$1 = \frac{\omega_{p+}^2}{\omega^2 - \omega_{c+}^2(1 + k_\perp^2 \rho_+^2)} + \frac{\omega_{p-}^2}{\omega^2 - \omega_{c-}^2(1 + k_\perp^2 \rho_-^2)}. \tag{2.13}$$

The LF ($\omega \lesssim \omega_{c\pm} \ll \omega_{p\pm}$) and long wavelength ($k_\perp \rho_\pm \ll 1$) assumptions lead to the solution of (2.13) as

$$\omega^2 = \omega_{c+}\omega_{c-} + \left(\frac{\delta + M}{1 + M}\right) k_\perp^2 V_{T+}^2. \tag{2.14}$$

This relation reveals that the LF sound mode described by the phase velocity (2.11*a–c*) is modified by constant cyclotron frequencies of both the ions and the phase velocity

https://doi.org/10.1017/S0022377820001348 Published online by Cambridge University Press

$\omega/k_\perp > V_p$. We call this mode the cyclotron mode in PINI plasma. In case of pure perpendicular propagation, we obtain $\omega \sim \sqrt{\omega_{c+}\omega_{c-}}$, lower hybrid type oscillation in PINI plasmas.

The above linear analysis clearly demonstrates that the PINI plasma model considered here is a coupled transverse–longitudinal complex dynamical system described by the set of fluid equations ((2.5)–(2.7)). The $\boldsymbol{E} \times \boldsymbol{B}$ term makes this coupling between the LF sound and cyclotron waves and thereby introduces complexity in the collective dynamics in PINI magnetized plasma. In such plasma

$$\Omega_- = M\Omega_+ = \Omega \text{ (say)}, \tag{2.15}$$

and therefore in the proceeding theoretical and numerical analysis, we use the notation of (2.15) instead of $\Omega_\pm$.

3. Weakly nonlinear LF wave dynamics

In the preceding section, we have seen that (like usual electron–ion plasma) the phase velocity of the cyclotron wave is greater than that of sound wave ($\omega/k_\perp > V_p$) in PINI plasmas and that then the ion velocity is, to a good approximation, along the z-direction, i.e. the direction of the external uniform magnetic field (Zakharov & Kuznetsov 1974). We introduce the slow space and time scales to study the weakly nonlinear dynamics of the LF ion sound wave as

$$\xi = \sqrt{\epsilon}(z - Vt), \quad \zeta = \epsilon x, \quad \eta = \epsilon y, \quad \tau = \epsilon^{3/2}t, \tag{3.1a–d}$$

where V is the normalized phase velocity of the ion sound wave and ϵ is a small parameter that characterizes the strength of nonlinearity (amplitude of the wave). The dynamical variables are expanded in powers of ϵ as

$$f = f_0 + \epsilon f^{(1)} + \epsilon^2 f^{(2)} + \cdots \quad \text{and} \tag{3.2}$$

where $f = n_\pm, v_{\pm z}, \phi; f_0 = 1$ for $n_\pm$ and 0 for other variables.

To study the effects of weak magnetic field, we consider the perturbation scaling as

$$\Omega = \Omega_0\sqrt{\epsilon}, \tag{3.3}$$

where Ω_0 is of the order of unity. Typically in laboratory PINI magnetized plasma $\Omega \sim 10^{-2}$. If Ω is not so small, we can still use the same scaling but now Ω_0 should be comparatively large, which does not present any hurdles to the subsequent analysis (Taniuti 1974).

Substituting the stretching coordinates (3.1*a–d*) and perturbation expansion (3.2) together with the scaling (3.3) into the basic equations ((2.5)–(2.7)), we obtain the following relations in the lowest powers of ϵ subject to the localized solution boundary conditions:

$$v_{\pm z}^{(1)} = Vn_\pm^{(1)}, \quad n_+^{(1)} = n_-^{(1)}, \quad MVv_{\pm z}^{(1)} = \pm\phi^{(1)} + \sigma_\pm n_\pm^{(1)}. \tag{3.4a–c}$$

This self-consistently determines the (normalized) phase velocity of the linear wave as

$$V = \sqrt{\frac{\sigma}{1+M}}, \quad \sigma = \sigma_+ + \sigma_-. \tag{3.5a,b}$$

In dimensional form, this (3.5*a*,*b*) can be written as

$$\frac{\omega}{k_\parallel} = \sqrt{\frac{\sigma}{1+M}}\sqrt{\frac{T}{m_-}} = \sqrt{\frac{T_+ + T_-}{m_+ + m_-}}, \tag{3.6}$$

https://doi.org/10.1017/S0022377820001348 Published online by Cambridge University Press

the same as the phase velocity of the LF ion sound wave in the limit ($k_{\parallel} \to 0$) (2.11*a–c*). The next highest order, (ϵ^2), yields

$$\left.\begin{aligned} MV\partial_\xi v_{+x}^{(1)} &= \partial_\zeta \phi^{(1)} - \Omega_0 v_{+y}^{(1)} + \sigma_+ \partial_\zeta n_+^{(1)}, \\ V\partial_\xi v_{-x}^{(1)} &= -\partial_\zeta \phi^{(1)} + \Omega_0 v_{-y}^{(1)} + \sigma_- \partial_\zeta n_-^{(1)}, \\ MV\partial_\xi v_{+y}^{(1)} &= \partial_\eta \phi^{(1)} + \Omega_0 v_{+x}^{(1)} + \sigma_+ \partial_\eta n_+^{(1)}, \\ V\partial_\xi v_{-y}^{(1)} &= -\partial_\eta \phi^{(1)} - \Omega_0 v_{-x}^{(1)} + \sigma_- \partial_\eta n_-^{(1)}, \end{aligned}\right\} \tag{3.7}$$

$$\partial_\xi^2 \phi^{(1)} = n_-^{(2)} - n_+^{(2)}. \tag{3.8}$$

From the relations in (3.7), we obtain

$$\left.\begin{aligned} \left(M^2V^2\partial_\xi^2 + \Omega_0^2\right) v_{+x}^{(1)} &= \left(MV^2\partial_{\xi\zeta} - \Omega_0\partial_\eta\right)\phi^{(1)} + \sigma_+\left(MV\partial_{\xi\zeta} - \Omega_0\partial_\eta\right) n_+^{(1)}, \\ \left(V^2\partial_\xi^2 - \Omega_0^2\right) v_{-x}^{(1)} &= -\left(V^2\partial_{\xi\zeta} + \Omega_0\partial_\eta\right)\phi^{(1)} + \sigma_-\left(V\partial_{\xi\zeta} + \Omega_0\partial_\eta\right) n_-^{(1)}, \end{aligned}\right\} \tag{3.9}$$

$$\left.\begin{aligned} \left(M^2V^2\partial_\xi^2 + \Omega_0^2\right) v_{+y}^{(1)} &= \left(MV^2\partial_{\xi\zeta} + \Omega_0\partial_\eta\right)\phi^{(1)} + \sigma_+\left(MV\partial_{\xi\zeta} + \Omega_0\partial_\eta\right) n_+^{(1)}, \\ \left(V^2\partial_\xi^2 - \Omega_0^2\right) v_{-y}^{(1)} &= -\left(V^2\partial_{\xi\zeta} - \Omega_0\partial_\eta\right)\phi^{(1)} + \sigma_-\left(V\partial_{\xi\zeta} - \Omega_0\partial_\eta\right) n_-^{(1)}. \end{aligned}\right\} \tag{3.10}$$

Finally, the highest order, ($\epsilon^{5/2}$), yields

$$\left.\begin{aligned} \partial_\tau n_+^{(1)} - V\partial_\xi n_+^{(2)} + \partial_\zeta v_{+x}^{(1)} + \partial_\eta v_{+y}^{(1)} + \partial_\xi v_{+z}^{(2)} + \partial_\xi\left(n_+^{(1)} v_{+z}^{(1)}\right) &= 0, \\ \partial_\tau n_-^{(1)} - V\partial_\xi n_-^{(2)} + \partial_\zeta v_{-x}^{(1)} + \partial_\eta v_{-y}^{(1)} + \partial_\xi v_{-z}^{(2)} + \partial_\xi\left(n_-^{(1)} v_{-z}^{(1)}\right) &= 0, \end{aligned}\right\} \tag{3.11}$$

$$\left.\begin{aligned} M\partial_\tau v_{+z}^{(1)} - MV\partial_\xi v_{+z}^{(2)} + \partial_\xi\phi^{(2)} + \sigma_+\partial_\xi n_+^{(2)} + Mv_{+z}^{(1)}\partial_\xi v_{+z}^{(1)} - \sigma_+ n_+^{(1)}\partial_\xi n_+^{(1)} &= 0, \\ \partial_\tau v_{-z}^{(1)} - V\partial_\xi v_{-z}^{(2)} - \partial_\xi\phi^{(2)} + \sigma_-\partial_\xi n_-^{(2)} + v_{-z}^{(1)}\partial_\xi v_{-z}^{(1)} - \sigma_- n_-^{(1)}\partial_\xi n_-^{(1)} &= 0. \end{aligned}\right\} \tag{3.12}$$

The combination of (3.8)–(3.12), yields the following weakly nonlinear evolution equation for LF sound wave in PINI magnetoplasmas:

$$\partial_\tau n^{(1)} + \alpha n^{(1)}\partial_\xi n^{(1)} + \beta\partial_\xi^3 n^{(1)} + \frac{V^3}{2(1+M)}\left[\frac{M^3}{\left(V^2M^2\partial_\xi^2 + \Omega_0^2\right)} + \frac{1}{\left(V^2\partial_\xi^2 + \Omega_0^2\right)}\right]\partial_\xi\nabla_{\zeta\eta}^2 n^{(1)} = 0, \tag{3.13}$$

which can also be recast in the form

$$\left(V^2M^2\partial_\xi^2 + \Omega_0^2\right)\left(V^2\partial_\xi^2 + \Omega_0^2\right)\left[\partial_\tau n^{(1)} + \alpha n^{(1)}\partial_\xi n^{(1)} + \beta\partial_\xi^3 n^{(1)}\right] + \frac{V^3}{2(1+M)}\left[M^3\left(V^2\partial_\xi^2 + \Omega_0^2\right) + \left(V^2M^2\partial_\xi^2 + \Omega_0^2\right)\right]\partial_\xi\nabla_{\zeta\eta}^2 n^{(1)} = 0, \tag{3.14}$$

where $\nabla_{\zeta\eta}^2 \equiv \partial_\zeta^2 + \partial_\eta^2$, the coefficient of nonlinearity (α) and the dispersive term (β) are given by

$$\alpha = \sqrt{\frac{\sigma}{1+M}} \quad \text{and} \quad \beta = \frac{\alpha}{2\sigma}\left(\frac{\sigma_+ - M\sigma_-}{1+M}\right)^2. \tag{3.15a,b}$$

To the best of our knowledge the (3.14) is novel in the PINI plasma literature. In the limit, M & $\sigma_- \to 0$, $V \to 1$ and we recover a similar equation derived for ion acoustic waves in

https://doi.org/10.1017/S0022377820001348 Published online by Cambridge University Press

presence of a weak magnetic field in an electron–ion plasma (Laedke & Spatschek 1982; Poria & Ghosh 2016) as

$$(\partial_\xi^2 + \Omega_0^2)[\partial_\tau n^{(1)} + n^{(1)}\partial_\xi n^{(1)} + \tfrac{1}{2}\partial_\xi^3 n^{(1)}] + \tfrac{1}{2}\partial_\xi \nabla_{\zeta\eta}^2 n^{(1)} = 0. \tag{3.16}$$

Thus the presence of lighter ion inertia and heavier ion thermal effects make the physical system more complex in a PINI plasma than that of the usual electron–ion plasma. In the absence of magnetic field ($\Omega_0 = 0$), we recover the Kadomtsev–Petviashvili equation (Kadomtsev & Petviashvili 1970) and in the strong magnetic field limit ($\Omega_0^2 \gg \partial_\xi^2$), we obtain an equation similar to the Zakharov–Kuznetsov equation (Zakharov & Kuznetsov 1974). Thus the derived nonlinear equation (3.14) is a general nonlinear equation, applicable for both magnetized and unmagnetized physical systems where such equations arise. The solutions of this equation are interesting, and applicable in different fields of physics and mathematics as described in the proceeding sections.

4. Phase-space analysis

The derived nonlinear equation (3.14) is not exactly integrable and therefore to investigate the nonlinear solutions of this equation, we consider a stationary plane wave frame (Witham 1999) of the form

$$\chi = k_\xi \xi + k_\eta \eta + k_\zeta \zeta - V_f \tau, \tag{4.1}$$

and transform (3.14) to this wave frame. Here V_f is the wave frame velocity and k_η, k_ζ, k_ξ, are the direction cosines so that $k_\eta^2 + k_\zeta^2 + k_\xi^2 = 1$. The velocity V_f is related to the Mach number ($\mathcal{M}$) in the following way. According to the stretching coordinate (3.1*a–d*), we have

$$\chi = \sqrt{\epsilon}\left[\sqrt{\epsilon}k_\eta y + \sqrt{\epsilon}k_\zeta x + k_\xi\left(z - (V + \epsilon V_f)t\right)\right]. \tag{4.2}$$

This clearly shows that the nonlinear wave velocity is $(V + \epsilon V_f)$ and consequently $\mathcal{M}$ is given by

$$\mathcal{M} = \frac{V + V_f}{V} = 1 + \epsilon\left(\frac{V_f}{V}\right) \Rightarrow V_f \propto (\mathcal{M} - 1)\,. \tag{4.3}$$

In the linear limit we recover $\lim_{\epsilon\to 0}\mathcal{M} = 1$.

Integrating the transformed equation once, we finally obtain the following nonlinear ordinary differential equation with $n^{(1)} \equiv X$:

$$\frac{\mathrm{d}^7 X}{\mathrm{d}\chi^7} + \frac{\mathrm{d}^5}{\mathrm{d}\chi^5}\left(f_1 X + \frac{f_4}{2}X^2\right) + \frac{\mathrm{d}^3}{\mathrm{d}\chi^3}\left(f_2 X + \frac{f_5}{2}X^2\right) + \frac{\mathrm{d}}{\mathrm{d}\chi}\left(f_3 X + \frac{f_6}{2}X^2\right) = 0, \tag{4.4}$$

where the coefficients $f_j (j = 1, \ldots, 6)$ are given in appendix A. In this transformed equation (4.4), we use the condition $k_\eta^2 + k_\zeta^2 = 1 - k_\xi^2$. Also (4.4) is a seventh-order nonlinear ordinary differential equation. To reduce the dimension of the trajectory in phase-space, we derive the first integral (I) of the above (4.4) in the χ frame, which reads as

$$I \equiv \frac{\mathrm{d}^6 X}{\mathrm{d}\chi^6} + \frac{\mathrm{d}^4}{\mathrm{d}\chi^4}\left(f_1 X + \frac{f_4}{2}X^2\right) + \frac{\mathrm{d}^2}{\mathrm{d}\chi^2}\left(f_2 X + \frac{f_5}{2}X^2\right) + X\left(f_3 + \frac{f_6}{2}X\right) = C. \tag{4.5}$$

According to the Galilean symmetry group (Arnold 1989), we choose $C = 0$ in (4.5) and construct the following sixth-order autonomous nonlinear dynamical system in the

https://doi.org/10.1017/S0022377820001348 Published online by Cambridge University Press

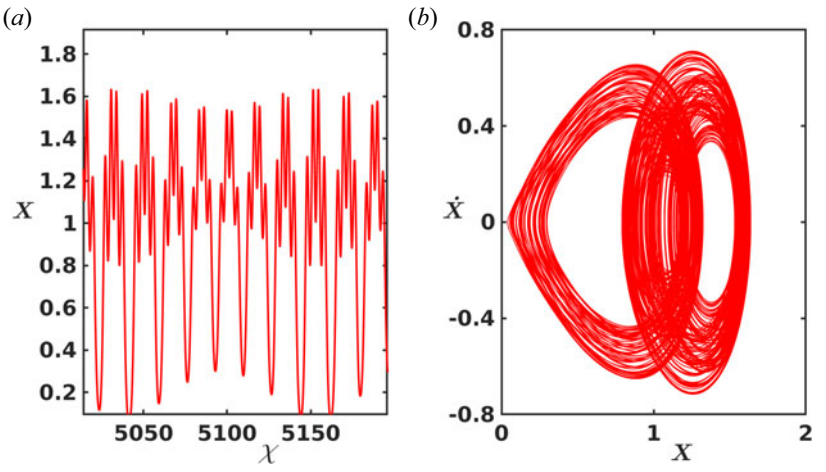


FIGURE 1. Numerical solution of the nonlinear system (4.6*a–c*) in the neighbourhood of c_0 for the parameters $\Omega_0 = 0.4$, $k_\xi = 0.85$ and $V_f = 0.4$.

χ frame:

$$\dot{\mathcal{F}} = \mathcal{G}; \quad \mathcal{F} = (X, Y, Z, W, R, Q)^T, \quad \mathcal{G} = (Y, Z, W, R, Q, F)^T, \tag{4.6a–c}$$

$$F = -f_1 R - f_2 Z - f_3 X - f_4\left(3Z^2 + 4YW + XR\right) - f_5\left(Y^2 + XZ\right) - f_6 X^2, \tag{4.7}$$

where dot $(\cdot)$ represents the derivative with respect to χ.

4.1. *Nonlinear analysis: numerical simulation*

Here, we analyse the nonlinear system (4.6*a–c*) by means of a numerical simulation to get insight of the complexity of the derived nonlinear evolution equation (3.14) in the χ frame. This system (4.6*a–c*) has two critical points in the sixth-dimensional phase space. However, we consider only the critical point $c_0 = (0, 0, 0, 0, 0, 0)$ as it corresponds to the equilibrium state of the PINI plasmas. We consider a small oscillation around c_0 and simulate the system (4.6*a–c*) with the help of a MATLAB-based Runge–Kutta–Fehlberg (known as RKF) computational method for the possible set of experimental parameters (Kim *et al.* 2013; Rosenberg & Merlino 2013): $B = 0.3T$, $n_+ = 1 \times 10^{15}$ m$^{-3} = n_-$, $T_+ = 0.2$ eV, $T_- = 0.026$ eV, $m_+/m_p = 39$ and $m_-/m_p = 350$. These parameters yield, $\omega_{p-} \approx 2.2 \times 10^6$ s^{-1}, $\omega_{p+} \approx 6.6 \times 10^6$ s^{-1}, $\rho_+ \approx 0.95$ mm, $\rho_- \approx 1$ mm, $\omega_{c+} \approx 7.3 \times 10^5$ rad s^{-1} and $\omega_{c-} \approx 8.2 \times 10^4$ rad s^{-1}. These values estimate $\Omega \approx 0.037$ which justifies the perturbation scaling (3.3).

The simulations are performed for a sufficiently long time (large span of χ $(0 \leq \chi \leq 10\,000)$) and we observed bounded solutions. However, for better clarity of the solutions (figures), we display the solutions for the subintervals of χ. The computational results are displayed graphically in figures 1–4.

The solution and the corresponding projection of phase-space trajectory for the parameters $V_f = 0.4$ and $k_\xi = 0.85$ (almost parallel) are displayed in figure 1. The curve in figure 1(*a*) shows that a small disturbance around c_0 develops into a multifrequency (finite) oscillation and the corresponding phase portrait in figure 1(*b*) shows the quasi-periodic nature of the solution.

The curves in the figures 2(*a*) and 3(*a*) for relatively large values of $V_f = 1$ and $V_f = 1.5$ reveal that the nonlinear oscillations are aperiodic and the amplitudes of the oscillations

https://doi.org/10.1017/S0022377820001348 Published online by Cambridge University Press

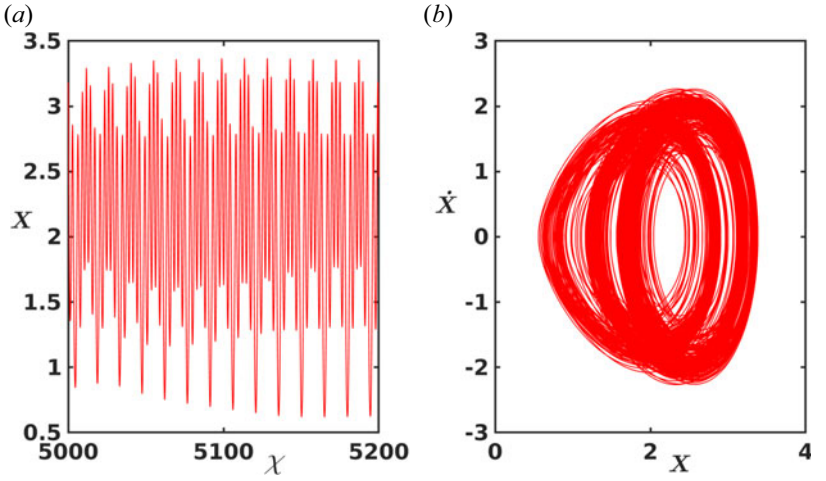


FIGURE 2. Numerical solution of the nonlinear system (4.6*a–c*) in the neighbourhood of c_0 for the parameters $\Omega_0 = 0.4$, $k_\xi = 0.85$ and $V_f = 1$.

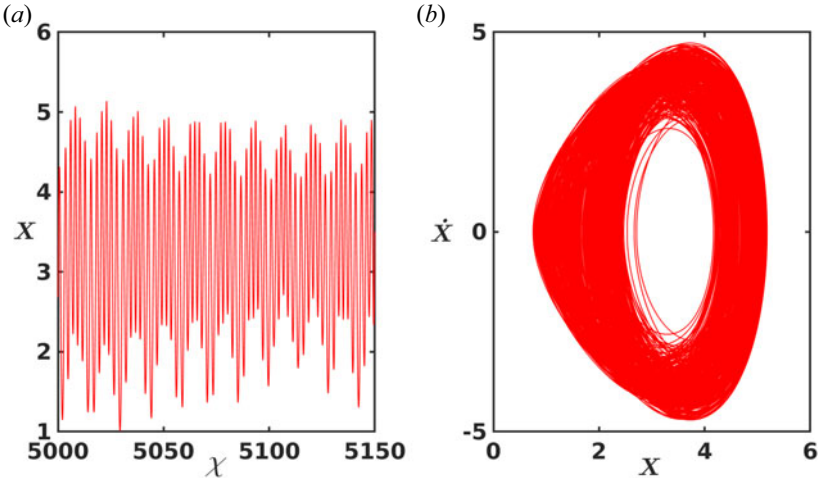


FIGURE 3. Numerical solution of the nonlinear system (4.6*a–c*) in the neighbourhood of c_0 for the parameters $\Omega_0 = 0.4$, $k_\xi = 0.85$ and $V_f = 1.5$.

are highly irregular. The corresponding phase portraits as depicted in figures 2(*b*) and 3(*b*) demonstrate the bounded, aperiodic and asymmetric nature of the solutions.

The result for relatively small value of $k_\xi = 0.7$ ($V_f = 1$) is displayed in figure 4(*a*,*b*). These figures show the qualitatively similar behaviour of the nonlinear wave. These numerical solutions demonstrate the chaotic behaviour of the weakly nonlinear wave in PINI plasma in the presence of an external magnetic field. Physically, increase in $\mathcal{M}$ (according to the relation (4.3), $V_f \propto (\mathcal{M} - 1)$) in the system (4.6*a–c*) enhances and creates new perturbations in the collective ion motions. This nonlinearity introduced by the Mach number $\mathcal{M}$ generates new harmonics, and the chaotic behaviour shows these strong harmonic generation phenomena.

https://doi.org/10.1017/S0022377820001348 Published online by Cambridge University Press

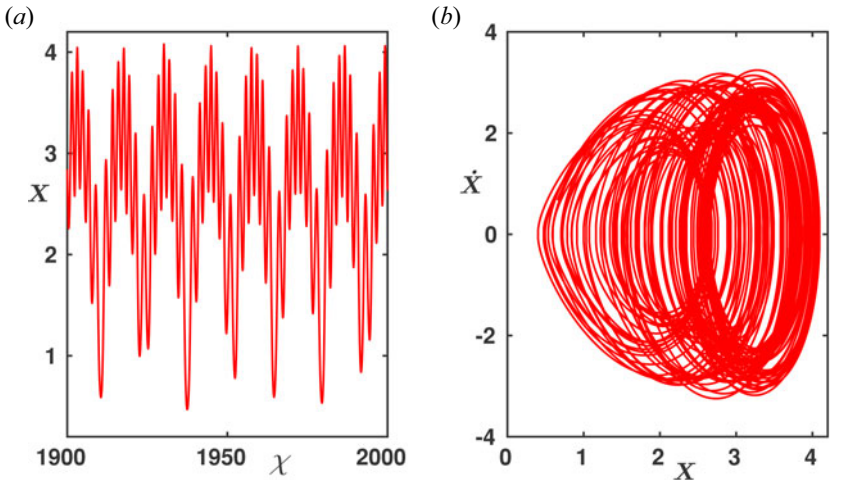


FIGURE 4. Numerical solution of the nonlinear system (4.6*a–c*) in the neighbourhood of c_0 for the parameters $\Omega_0 = 0.4$, $k_\xi = 0.7$ and $V_f = 1$.

The comparison between the solutions presented in figures 1–3 clearly demonstrates that the wave amplitudes increase with the increase of the value of V_f (i.e. $\mathcal{M}$). In a similar way, the comparison between the solutions in figures 2 and 4 reveal that the wave amplitudes decrease according to the decrease in the value of k_ξ. Furthermore, for the proper identification of different solutions of the system (4.6*a–c*), we perform a Poincarè return map analysis in the next section.

4.2. *Poincarè return map analysis*

It is well known that the Poincarè return map is a very powerful tool (Lorenz 1963; Molenaar *et al.* 2005) used to analyse the qualitative behaviour of a higher-dimensional dynamical system. Thus to confirm the observed numerical solutions (quasi-periodic and chaotic) of a nonlinear wave, we apply the Poincarè return map analysis and construct the one-dimensional return map

$$X_{n+1} = H(X_n) \tag{4.8}$$

from the time (χ) series data of the variable X. To construct this return map, we collect the local maxima of X in such a way that the $(n+1)$th local maxima X_{n+1} of X is a function H of the nth local maxima X_n. For the determination of the nature of the dynamical behaviour of the nonlinear system (4.6*a–c*), we plot the first return map constructed with the series of the maxima of the variable X in figures 1–4. The first return map corresponding to the time (χ) evolution of figure 1 is displayed in figure 5(*a*). Similarly, the return maps corresponding to the time evolution of figures 2, 3 and 4 are displayed in figures 5(*b*), 5(*c*) and 5(*d*), respectively.

Figure 5(*a*) demonstrates that points are densely populated and lie on smooth closed curves. There exists multiple closed curves which indicate multifrequency (finite) oscillation and confirm the existence of quasi-periodic structures of the nonlinear wave as shown in figure 1. In case of figure 5(*b–d*), the points are densely scattered and lie on a single island. Moreover, all these figures exhibit irregular distributions of points without any known pattern. Such first-return maps are characteristic of chaotic oscillations (Lorenz 1963; Molenaar *et al.* 2005) and thereby confirm the existence of chaotic behaviour of the weakly nonlinear wave in PINI magnetoplasma as shown in figures 2–4.

https://doi.org/10.1017/S0022377820001348 Published online by Cambridge University Press

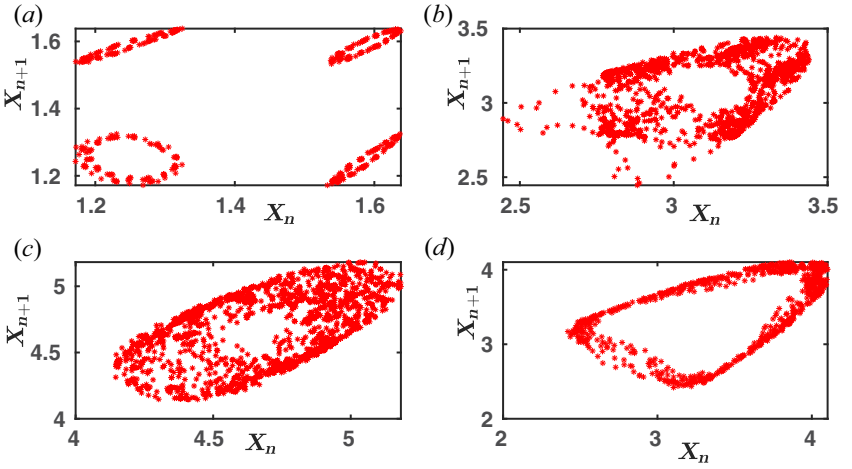


FIGURE 5. Poincarè return map of the X variable (i.e. the number density). Panel (a–d) represent the return map corresponding to figures 1–4.

5. Discussions

In the present work, we investigate the macroscopic dynamics of a weakly nonlinear, LF sound wave in an experimentally developed PINI plasma (Intrator *et al.* 1983; Kim & Merlino 2007; Merlino & Kim 2008; Kim *et al.* 2013; Rosenberg & Merlino 2013) in the presence of an external uniform weak magnetic field. We consider fluid descriptions of each ion for the collective dynamics of such PINI plasmas (Intrator *et al.* 1983). The linear mode analysis for LF and long wavelength disturbances reveal that PINI magnetoplasma sustains sound waves (longitudinal oscillation) and cyclotron waves (transverse oscillations). It is necessary to have the condition $\sqrt{T_-/T_+} \ll \sqrt{m_-/m_+}$ for the fluid descriptions of both the ion species in PINI plasmas; otherwise, the wave–particle resonances occur and the LF modes suffer strong Landau damping. In PINI plasma experiments (Intrator *et al.* 1983; Kim *et al.* 2013; Rosenberg & Merlino 2013), this analytic limit is marginally satisfied.

A novel nonlinear partial differential equation (3.14) is derived that governs the dynamics of the nonlinear wave. This nonlinear equation is analysed analytically and numerically with the help laboratory plasma parameters. The analysis is performed on a plane wave frame by posing the nonlinear problem as a six-dimensional autonomous nonlinear dynamical system. The results reveal that in the presence of a magnetic field, the weakly nonlinear wave exhibits a wide class of periodic and aperiodic nonlinear structures.

The numerical simulations confirm that the nonlinear wave exhibits quasi-periodic structures for low Mach number. However, with the increase of the Mach number, quasi-periodic structure breaks. Instead, bounded, aperiodic and irregular oscillations appear for $\mathcal{M} \sim 2$ and $\mathcal{M} \sim 2.5$. These structures demonstrate the chaotic dynamics of the nonlinear wave in PINI magnetized plasma. Later, Poincarè return map analysis confirms the observed quasi-periodic and chaotic structures of the nonlinear wave. The external static magnetic-field induced Lorentz force ($\boldsymbol{E} \times \boldsymbol{B}$) introduces the complexity in PINI plasma and makes the collective dynamics chaotic. In the simulation, it is also observed that the amplitude of the nonlinear wave depends (increases with the increase of $\mathcal{M}$ and k_ξ) on both the Mach number and the direction of propagation of the wave.

Chaos is a characteristic of a nonlinear system. This chaotic motion gives rise to the diffusion of energy and leads to the establishment of the energy spectrum – the

https://doi.org/10.1017/S0022377820001348 Published online by Cambridge University Press

signature of stochastic phenomena. These phenomena cause stochastic heating of plasma (Karney & Bers 1977). Chaos generated through wave–particle interactions is responsible for the plasma heating (Lichtenberg & Lieberman 1992). However, the result of the present investigation reveals that the weakly nonlinear (wave–wave) interactions between (relatively high-frequency) cyclotron waves and (LF) sound waves lead to the chaotic dynamics for relatively large Mach number. Physically, increase in wave amplitude (Mach number) enhances and creates new perturbations in the collective ion motions that generates new harmonics. These harmonics interact among themselves (many wave interactions) and form coherence structures, which for suitable physical parameters show chaotic dynamics (Sirovich 1989). As a result, the observed chaos due to wave–wave interactions could also be a viable physical mechanism for the plasma heating.

Moreover, in the case of equal mass ($m_- = m_+ = m$), the dispersion relation (2.9) yields

$$\omega \cong k_\parallel V_s, \quad V_s = \sqrt{T/m}; \quad T = (T_+ + T_-)/2, \tag{5.1a–c}$$

the phase velocity of ion acoustic wave as observed in equal mass pair-ion laboratory plasmas (Oohara & Hatakeyama 2005). Similarly, from dispersion relation (2.14) we obtain

$$\omega^2 = \omega_c^2 + k_\perp^2 V_s^2, \tag{5.2}$$

the dispersion relation of the ion cyclotron wave in equal mass pair-ion plasma.

Lastly, the numerical simulations are performed on the basis of real experimental parameters. Thus we can expect that the results in this manuscript will help to conduct experiments on nonlinear features in PINI magnetoplasma. Until now, we have not encountered any experimental observations of nonlinear LF waves in PINI magnetoplasma. However, we hope that the predicted complex structures such as quasi-periodicity and chaos will be observed in future planed PINI magnetoplasmas.

Acknowledgements

The authors would also like to thank two referees for their careful reading and the offering of constructive suggestions to help improve the manuscript.

Editor Edward Thomas thanks the referees for their advice in evaluating this article.

Declaration of interests

The authors report no conflict of interest.

Appendix A. Coefficients in the nonlinear system (4.6*a–c*)

$$f_1 = \frac{1}{k_\xi^2}\left[\frac{\Omega_0^2}{V^2} + \frac{f_4\left(V(1-k_\xi^2) - 2V_f k_\xi\right)}{2V} + \frac{\Omega_0^2 V^2}{(\sigma - V^2)^2}\right]. \tag{A 1}$$

$$f_2 = \frac{\Omega_0^2}{k_\xi^6 V^2}\left[\frac{(1-k_\xi^2)(\sigma - V^2)}{(V^2 - \sigma_-)^2}\left(1 - \frac{V^6}{(\sigma - V^2)^3}\right) + \frac{\Omega_0^2 V^2 k_\xi^2}{(\sigma - V^2)^2} - \frac{f_5 V k_\xi^5}{\Omega_0^2}\right]. \tag{A 2}$$

$$f_3 = -\frac{2V_f f_6}{k_\xi V}, \quad f_4 = \frac{2\sigma}{k_\xi^2 (V^2 - \sigma_-)^2}, \quad f_5 = \frac{\Omega_0^2 f_4}{k_\xi^2 V^2}\left(1 + \frac{V^4}{(\sigma - V^2)^2}\right). \tag{A 3a–c}$$

$$f_6 = \frac{\Omega_0^4 f_4}{2k_\xi^4 (\sigma - V^2)^2}. \tag{A 4}$$

https://doi.org/10.1017/S0022377820001348 Published online by Cambridge University Press

REFERENCES

ADAK, A., GHOSH, S. & CHAKRABARTI, N. 2015 Ion acoustic shock wave in collisional equal mass plasma. *Phys. Plasmas* **22**, 102307.

ARNOLD, V. I. 1989 *Mathematical Methods of Classical Mechanics*. Springer.

ECONOMOU, D. J. 2007 Fundamentals and applications of ion–ion plasmas. *Appl. Surf. Sci*. **253**, 6672–6680.

GHOSH, S., ADAK, A. & KHAN, M. 2014 Dissipative solitons in pair-ion plasmas. *Phys. Plasmas* **21**, 12303.

GREAVES, R. G. & SURKO, C. M. 2000 Inward transport and compression of a positron plasma by a rotating electric field. *Phys. Rev. Lett*. **85**, 1883–1886.

INTRATOR, T., HERSHKOWITZ, N. & STERN, R. 1983 Beam–plasma interactions in a positive ion–negative ion plasma. *Phys. Fluids* **26**, 1942–1948.

IWAMOTO, N. 1993 Collective modes in nonrelativistic electron-positron plasmas. *Phys. Rev.* E **47**, 604–611.

KADOMTSEV, B. B. & PETVIASHVILI, V. I. 1970 On the stability of solitary waves in weakly dispersing media. *Sov. Phys. Dokl*. **15**, 539–541.

KARNEY, C. F. F. & BERS, A. 1977 Stochastic ion heating by a perpendicularly propagating electrostatic wave. *Phys. Rev. Lett*. **39**, 550–554.

KELLY, M. C. & HEELIS, R. A. 1989 *The Earth's Ionosphere: Plasma Physics and Electrodynamics*. Academic Press.

KIM, S. H., HENRICH, J. R. & MERLINO, R. L. 2008 Electrostatic ion-cyclotron waves in a plasma with heavy negative ions. *Planet. Space Sci*. **56**, 1552–1559.

KIM, S. H. & MERLINO, R. L. 2007 Electron attachment to C_7F_{14} and SF_6 in a thermally ionized potassium plasma. *Phys. Rev.* E **76**, 035401.

KIM, S. H., MERLINO, R. L., MEYER, J. K. & ROSENBERG, M. 2013 Low-frequency electrostatic waves in a magnetized, current-free, heavy negative ion plasma. *J. Plasma Phys*. **79**, 1107–1111.

KOURAKIS, I., VERHEEST, F. & CRAMMER, N. F. 2007 Nonlinear perpendicular propagation of ordinary mode electromagnetic wave packets in pair plasmas and electron-positron-ion plasmas. *Phys. Plasmas* **14**, 022306.

LAEDKE, E. W. & SPATSCHEK, K. H. 1982 Nonlinear ion-acoustic waves in weak magnetic fields. *Phys. Fluids* **25**, 985–989.

LICHTENBERG, A. J. & LIEBERMAN, M. A. 1992 *Regular and Chaotic Dynamics*. Springer.

LORENZ, E. N. 1963 Deterministic nonperiodic flow. *J. Atmos. Sci*. **20**, 130–141.

MAITY, B., GHOSH, S. & BHARUTHRAM, R. 2015 Nonlinear ion acoustic wave in a pair-ion plasma in a uniform weak magnetic field. *Phys. Scr*. **90**, 045604.

MERLINO, R. L. & KIM, S. H. 2008 Measurement of the electron attachment rates for SF6 and C7F14 at Te = 0.2eV in a magnetized *Q* machine plasma. *J. Chem. Phys*. **129**, 224310.

MOLENAAR, D., CLERCX, H. J. H. & VAN HEIJST, G. J. F. 2005 Transition to chaos in a confined two-dimensional fluid flow. *Phys. Rev. Lett*. **95**, 104503.

MOSLEM, W. M., KOURAKIS, I. & SHUKLA, P. K. 2007 Finite amplitude envelope solitons in a pair-ion plasma. *Phys. Plasmas* **14**, 032107.

OOHARA, W. & HATAKEYAMA, R. 2005 Electrostatic waves in a paired fullerene-ion plasma. *Phys. Rev. Lett*. **95**, 175003.

PORIA, S. & GHOSH, S. 2016 Chaotic behavior of collective ion dynamics in the presence of an external static magnetic field. *Phys. Plasmas* **23**, 062315.

RATCLIFFE, J. A. 1972 *An Introduction to the Ionosphere and Magnetosphere*. Cambridge University Press.

ROSENBERG, M. & MERLINO, R. L. 2009 Instability of higher harmonic electrostatic ion cyclotron waves in a negative ion plasma. *J. Plasma Phys*. **75**, 495–508.

ROSENBERG, M. & MERLINO, R. L. 2013 Drift instability in a positive ion–negative ion plasma. *J. Plasma Phys*. **79**, 949–952.

https://doi.org/10.1017/S0022377820001348 Published online by Cambridge University Press

SHUKLA, P. K., BINGHAM, R., PHELPS, A. D. R. & STENFLO, L. 2009 Dark and grey electromagnetic electron-cyclotron envelope solitons in an electron-positron magnetoplasma. *J. Plasma Phys*. **75**, 575–580.

SHUKLA, P. K., ELIASSON, B. & STENFLO, L. 2011 Electromagnetic solitary pulses in a magnetized electron-positron plasma. *Phys. Rev.* E **84**, 037401.

SIROVICH, L. 1989 Chaotic dynamics of coherent structures. *Physica* D **37**, 126–145.

STENFLO, L., SHUKLA, P. K. & YU, M. Y. 1985 Nonlinear propagation of electromagnetic waves in magnetized electron-positron plasmas. *Astrophys. Space Sci*. **117**, 303–308.

STROGATZ, S. H. 1994 *Nonlinear Dynamics and Chaos: with applications to Physics, Biology, Chemistry and Engineering*. Addision-Wesley Publishing Company.

TANIUTI, T. 1974 Reductive perturbation method and far fields of wave equations. *Suppl. Prog. Theor. Phys*. **55**, 1–35.

WITHAM, G. B. 1999 *Linear and Nonlinear Waves*. John-Wiley and Sons.

YU, M. Y., SHUKLA, P. K. & STENFLO, L. 1986 Alfven vortices in a strongly magnetized electron – positron plasma. *Astrophys. J. Lett*. **309**, L63–L66.

ZAKHAROV, V. E. & KUZNETSOV, E. A. 1974 Three-dimensional solitons. *Sov. Phys. JETP* **39**, 285–286.

ZANK, G. P. & GREAVES, R. G. 1995 Linear and nonlinear modes in nonrelativistic electron-positron plasmas. *Phys. Rev.* E **51**, 6079–6090.

https://doi.org/10.1017/S0022377820001348 Published online by Cambridge University Press